Journal of the European Ceramic Society 21 (2001) 2037–2040

www.elsevier.com/locate/jeurceramsoc

Synthesis and electrical conductivity of $Y_{1-x}Mn_{1-y}O_{3-\delta}$

G. Lescano [a,b], F.M. Figueiredo [a,c], F.M.B. Marques [a,*], J. Schmidt [b]

[a] *Ceramics and Glass Engineering Department, UIMC, University of Aveiro, 3810-193 Aveiro, Portugal*
[b] *Chemistry Department, Universidad Nacional del Sur, 8000 Bahía Blanca, Argentina*
[c] *Science and Technology Department, Universidade Aberta, R. Escola Politécnica, 147 1269-001 Lisboa, Portugal*

Received 4 September 2000; received in revised form 23 October 2000; accepted 30 October 2000

Abstract

$YMnO_3$-related materials [stoichiometric (Y/Mn = 1), and Y or Mn deficient] were synthesized by a traditional ceramic route. Dense pellets obtained after sintering at different temperatures (1400–1500°C) were characterized by XRD, SEM/EDS, dilatometry (up to 1270°C) and dc electrical conductivity measurements in air (between 200 and 1000°C). The electrical conductivities of all compositions were close to each other and within the range 10^{-4} S/cm at about 200°C to 1 S/cm at about 1000°C. Arrhenius plots show three different slopes with smooth transitions around 300–350°C and 600–650°C. The activation energy increases from about 50 kJ/mol below 300°C to about 90 kJ/mol between 650 and 1000°C. XRD, SEM/EDS and thermal expansion measurements provided enough evidence on phase and mechanical stability constraints, thus questioning potential technological applications.

Keywords: Electrical conductivity; Perovskite; Thermal expansion; Yttrium manganite

1. Introduction

Oxide materials with a perovskite-type structure (ABO_3, A = La or Y, B = Mn, Co, Fe or Cr) deserved large attention in the past namely for considering possible applications as electrode or interconnect materials for solid oxide fuel cells (SOFCs). A-site doping with Sr or Ca and several combinations of transition metals in the B-site were exploited to try to improve the electrical conductivity and the electrocatalytic properties, to adjust the thermal expansion to those of potential electrolyte materials, or even to try to increase the chemical compatibility between electrode and electrolyte.[1–3] Previous studies on manganites (B = Mn) were dedicated mainly to doped samples but included also A-site substoichiometric materials.[1–3] The designation "stoichiometric material" will be used throughout this work to describe full occupancy of both cation sites (A/B = 1).

Yttrium manganite shows ferroelectric behavior with high T_C (> 600°C), being a p-type semiconductor in air, with low electronic conductivity at room temperature.[4] No structural changes could be identified by XRD at the ferroelectric–paraelectric phase transition temperature.[5] Previous attempts to try to design the electrical properties of $YMnO_3$ envisaged only room temperature applications and involved the exploitation of A-site doping and substoichiometry.[6,7] The synthesis of these materials deserved significant attention because of the formation of different phases with limited stability ranges apparently responsible for frequent cracking of samples.[7,8]

In $YMnO_3$, Y- or Mn-substoichiometry should be compensated by formation of electron holes or oxygen vacancies, depending on the relative energies for defect formation. This attempt to design the materials high-temperature electrical properties will be the central subject of attention in this work. Based on previous activity on this system suggesting limited ranges of substoichiometry,[6] three compositions were selected for the present study with Y/Mn ratios of 0.95/1 ($Y_{0.95}MnO_{3-\delta}$), 1/1 ($YMnO_{3-\delta}$) and 1/0.97 ($YMn_{0.97}O_{3-\delta}$). A combined study on structure, microstructure, thermal and high-temperature electrical properties of these materials is now reported for the first time.

* Corresponding author. Tel.: +351-234-370269; fax: +351-234-425300.
E-mail address: fmarques@cv.ua.pt (F.M.B. Marques).

0955-2219/01/$ - see front matter
PII: S0955-2219(01)00111-X

2. Experimental

Y_2O_3 (Aldrich) and $C_{10}H_{14}MnO_4$ (Manganese II acetylacetonate from Fluka) powders were used as starting materials. After mixing in appropriate proportions to obtain the envisaged Y/Mn ratios, the powders were ball milled for 2 h in ethanol using zirconia balls. After drying, calcination took place at 1100°C for 10 h. The materials were ball milled again under the same conditions and pressed into pellets of about 1 cm diameter prior to sintering at three different temperatures (for 5 h at 1400 and 1450°C, and for 2 h at 1500°C) in air, with a heating rate of 10°C/min.

Powders calcined at 1100°C and sintered samples were characterized by X-ray diffraction (XRD). The microstructure of sintered samples was observed by scanning electron microscopy (SEM) after polishing and thermal etching at temperatures 10% lower than the sintering temperature. Energy dispersive spectroscopy (EDS) was used to identify the chemical composition of different phases observed by SEM. Thermal expansion measurements were performed in air from room temperature to 1270°C with a constant heating rate of 10°C/min.

Electrical conductivity measurements were performed in the temperature range 200–1000°C using the four probe van der Pauw technique.[9] To perform these measurements four Pt electrodes are placed in contact with the pellet to drive the current and to read the voltage drop. The bulk conductivity can be determined when the following conditions are satisfied: (i) the contacts are at the circumference of the sample; (ii) the contacts are sufficiently small; (iii) the sample is of uniform thickness; (iv) the surface of the sample is singly connected, i.e. the sample must be homogeneous and without isolated holes.

3. Results and discussion

Fig. 1 shows a selected 2θ range of the XRD patterns of samples with nominal Y/Mn ratios of 1/1, 1/0.97 and 0.95/1 after treatment at 1100°C (Fig. 1A) and 1400°C (Fig. 1B). This 2θ range was selected for including the three largest peaks of $YMnO_3$ (file JCPDS No. 25-1079) and YMn_2O_5 (JCPDS file No. 34-0667), besides other smaller peaks of these phases. Both phases have large relevance for the following discussion.

XRD data of powder mixtures fired at 1100°C for 10 h shows the hexagonal $YMnO_3$ phase as well as YMn_2O_5. At 1400°C most lines can be assigned to the $YMnO_3$ perovskite. The peaks of YMn_2O_5 completely disappeared in agreement with the reported formation of this phase only within a limited range of temperatures (from about 840 to 1200°C) during the synthesis of $YMnO^3$.[8] Small unidentified peaks, presumably corresponding to residual amounts of several oxides (Y_2O_3, Mn_2O_3 and/or Mn_3O_4), were present in all compositions. This was observed in powders fired at 1100°C, in slowly cooled samples after sintering at 1400, 1450 and 1500°C, and also in one sample quenched in air from about 1300°C to room temperature. High temperature XRD was carried out with a stoichiometric sample (Y/Mn ratio 1/1). No evidence was found for structural changes corresponding to the ferroelectric–paraelectric transition, in agreement with results mentioned in previous work.[4]

SEM micrographs of samples sintered at 1400°C with Y/Mn ratios of 1/1, 1/0.97 and 0.95/1 revealed a dense microstructure with low porosity. These thermally etched samples showed also the presence of microcracks and secondary phases. One representative example of these microstructures is shown in Fig. 2. Combined SEM/EDS analysis showed the presence of manganese rich secondary phases consisting of grains with a diameter of about 1 μm between the larger perovskite grains. The formation of such secondary phases was observed in all compositions irrespective of thermal etching, and also in special series of samples fired at 1400°C for 15 h or following repeated calcination and ball milling steps. No evidence could be found for the presence of yttrium-rich phases, contrary to the expectation from nominal compositions.

Cracks were found in all thermally etched samples irrespective of the cooling rate. However, samples without

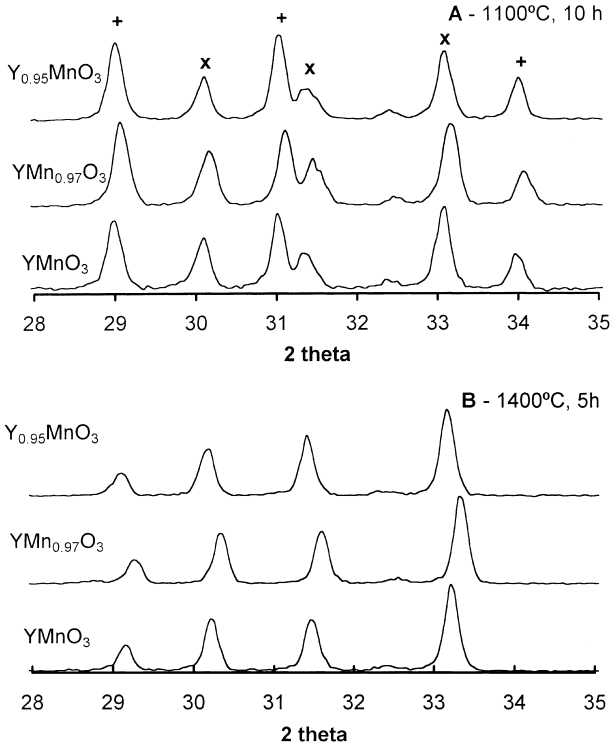

Fig. 1. XRD patterns of samples fired at different temperatures. Only the three major peaks of $YMnO_3$ and YMn_2O_5 are marked with the symbols × and +, respectively.

thermal etching were found free of cracks (Fig. 3), suggesting that the low temperature treatment (thermal etching at 1260°C) was essential for the development of such cracks. This fact, already reported in the literature,[7] will be discussed in further detail in the following paragraphs.

Contrast between phases is not clear in the sample shown in Fig. 3 due to the absence of thermal etching, but reasonably large and continuous areas suggest the presence of a liquid phase. Thermal etching would favor the crystallization of such a liquid and formation of new phases, as found in etched samples. This might also explain the absence of cracks in samples without any thermal treatment besides sintering.

Thermal expansion results obtained with all samples are shown in Fig. 4. In the case of stoichiometric samples (Y/Mn = 1/1) two slight changes in slope can be noticed at about 850 and close to 1200°C. In the case of the remaining samples only sharp changes can be noticed around 1200°C. Previous work suggested that $YMnO_3$ might decompose partly to YMn_2O_5 and Y_2O_3 at 840°C with oxygen release, or that residual amounts of yttrium and manganese oxides might combine with oxygen to form YMn_2O_5. At 1200°C YMn_2O_5 decomposes into $YMnO_3$ and Mn_2O_3, with oxygen release.[8] Published thermal gravimetric analysis (TGA) data suggests that slight oxygen uptake at about 840°C is possible (there is no evidence for any weight loss). Also, oxygen release at 1200°C is coherent with a sharp shift in TGA curves at this temperature.[7] Lastly, the transition between tetragonal and cubic Mn_3O_4 occurs at about 1175°C with a thermal hysteresis in the range of 25–75°C, and at about 900°C Mn_2O_3 transforms to Mn_3O_4 (tetragonal) with oxygen release.[10] Joint analysis of thermal performance now reported and published data supports the presence of Mn-rich phase(s): manganese oxide, YMn_2O_5 or both.

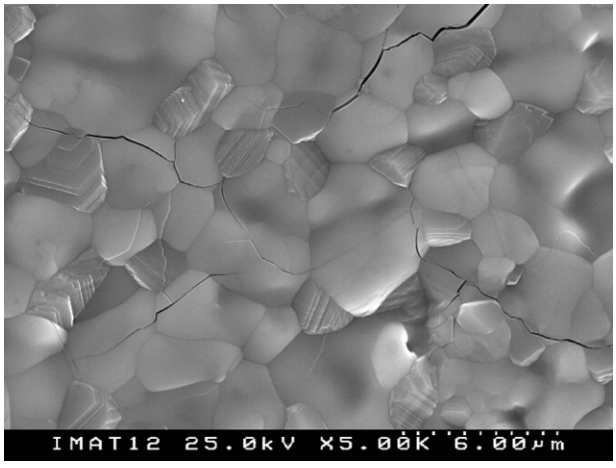

Fig. 2. Microstructure of one sample of $YMnO_3$ (with nominal Y/Mn ratio of 1) fired at 1400°C after polishing and thermal etching. Large grains fit the perovskite composition while small grains were found richer in Mn. Cracks are present everywhere after thermal etching.

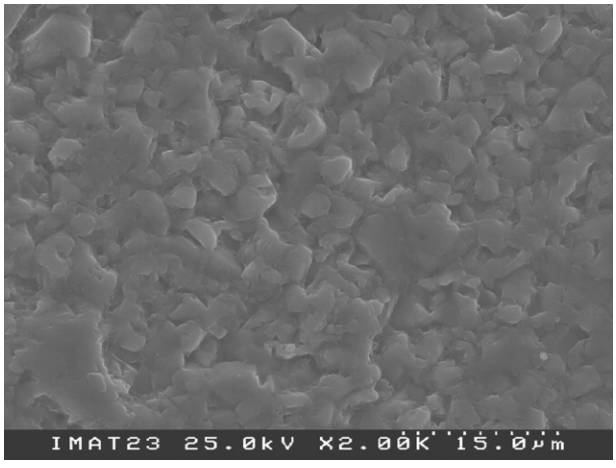

Fig. 3. Microstructure of one sample of $YMnO_3$ (with nominal Y/Mn ratio of 1/1) fired at 1400°C without thermal etching. No cracks can be noticed.

Pellets of all compositions sintered at 1400 and 1450°C for 5 h, and with a Y/Mn ratio of 1/1 sintered at 1500°C for 2 h, were used to perform dc conductivity measurements. A typical set of data (sintering temperature of 1400°C) is presented in Fig. 5 with all compositions following the same trend above 350°C. Overall, the conductivity values were close to 1 S cm^{-1} at 1000°C and around 10^{-4} S cm^{-1} at about 200°C. These values are more than one order of magnitude higher than those reported by Rao et al.[4] for $YMnO_3$, and two orders of magnitude lower than those mentioned by Fu et al. for $Y_{1-x}Sr_xMnO_3$.[8] The latter discrepancy is easily explained by the well known impact of A-site doping with Sr on the electrical conductivity of these perovskites.

Arrhenius plots are apparently broken around 600–650°C and at about 350°C. Activation energies were calculated from the classical relation $\sigma = \sigma_o \exp(E_a/RT)$. The activation energy increases from about 50 kJ/mol under 300°C to about 90 kJ/mol between 650 and 1000°C, depending slightly on composition. These changes in slope are coherent with previously reported data.[4] The

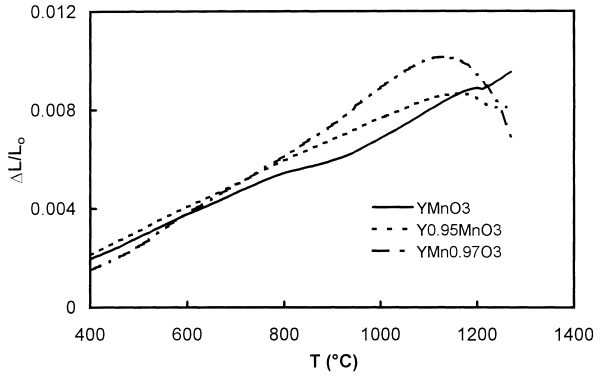

Fig. 4. Thermal expansion of sintered pellets of all compositions as a function of temperature.

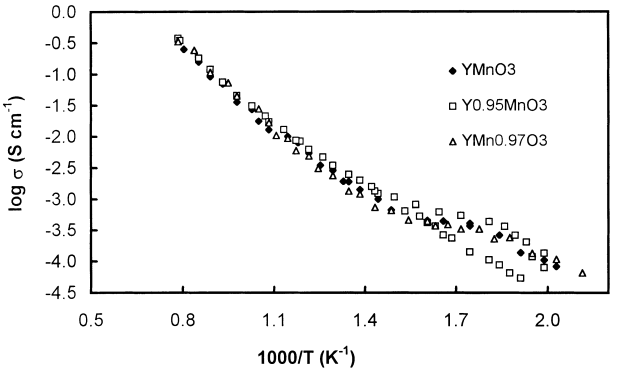

Fig. 5. Dependence of electrical conductivity on temperature for all materials sintered at 1400°C. Hysteresis between heating and cooling can be noticed in the case of the A-site deficient material.

high temperature shift in slope (around 600–650°C) is likely to be related to the ferroelectric–paraelectric transition, but there is no justification for the lower temperature effect either from XRD or thermal expansion data. One possibility is a change in the contribution of Mn-rich secondary phases to the overall conductivity, as secondary phases along the grain boundaries tend to dominate the low temperature electrical performance.

Hysteresis between heating and cooling can be seen in the case of the sample with a Y/Mn ratio of 0.95/1 (Fig. 5), the only nominal composition with Mn excess. This was the most pronounced effect observed amongst all samples and is again coherent with the presence of a Mn-rich phase along the grain boundaries, slowly equilibrating with oxygen at low temperatures.

XRD patterns of samples after conductivity measurements suggested the presence of manganese oxides and YMn_2O_5 besides the perovskite. This means that the transformations observed during thermal etching are also likely to occur during high temperature conductivity measurements.

All information suggests the likely presence of cracks and secondary phases disturbing the quality of the conductivity measurements. However, overlap between sets of data at high temperature and changes in slope close to the ferroelectric-paraelectric transition temperature also suggest that this behavior is characteristic to all these materials irrespective of small compositional differences and defects, thus corresponding to the intrinsic performance of these materials. Thus, formation of secondary phases and/or ionic defects to balance the nominal cation deficiency, with little effect on the concentration of small polarons (localized in Mn positions), are the most likely explanations for the present results. Overall, the electrical performance was clearly poor as potential electrode materials for SOFCs.

Single phase materials with the nominal compositions previously presented were not obtained (or at least were unstable after thermal treatment). The difficulties now reported are by no means unique. Previous work on this system including microstructural characterization is full of references to sample cracking.[7,8] A deep study on phase stability is thus necessary before consideration of any type of applications.

4. Conclusions

Different sintering conditions and nominal deviations from stoichiometry (Y/Mn = 1) showed no major effect on the high temperature electrical performance of $YMnO_3$-based materials. In particular, substoichiometry had no effect when compared to the known conductivity enhancement due to A-site doping with alkaline earth metals. Problems identified with the stability of these materials suggest limited potential for technological applications.

Acknowledgements

Financial support from the Programs ALFA (CEC, Brussels) and PRAXIS (FCT, Portugal), and UNS (Argentina) is greatly appreciated.

References

1. Takeda, Y., Kanno, R., Noda, M., Tomida, Y. and Yamamoto, O., Cathodic polarization phenomena of perovskite oxide electrodes with stabilized zirconia. *J. Electrochem Soc.*, 1987, **134**, 2656–2661.
2. Takeda, Y., Nakai, S., Kojima, T., Imanishi, N., Shen, G. Q., Yamamoto, O., Mori, M., Asakawa, C. and Abe, T., Phase Relation in the System $(La_{1-x}A_x)_{1-y}MnO_{3+z}$ (A = Sr and Ca). *Mater Res. Bull.*, 1991, **26**, 153–162.
3. Hammouche, A., Siebert, E. and Hammou, A., Crystallographic, thermal and electrochemical properties of the system $La_{1-x}Sr_xMnO_3$ for high temperature solid electrolyte cells. *Mater. Res. Bull.*, 1989, **24**, 367–380.
4. Rao, C. N. R., Rao, G. V. S. and Wanklyn, B. M., Electrical transport in rare-earth ortho-chromites, manganites and ferrites. *J. Phys. Chem. Solids*, 1971, **32**, 345–358.
5. Lukaszewicz and Karut-Kalicinska, J., X-ray investigations of the crystal structure and phase transitions of $YMnO_3$. *Ferroelectrics*, 1974, **7**, 81–82.
6. Shimura, T., Fujimura, N., Yamamori, S., Yoshimura, T. and Ito, T., Effects of stoichiometry and A-site substitution on the electrical properties of ferroelectric $YMnO_3$. *Jpn. J. Appl. Phys.*, 1998, **37**, 5280–5284.
7. Moure, C., Fernandez, J. F., Villegas, M. and Duran, P., Non-ohmic behaviour and switching phenomena in $YMnO_3$-based ceramic materials. *J. Eur. Ceram. Soc.*, 1999, **19**, 131–137.
8. Fu, B. and Huebner, W., Synthesis and properties of strontium-doped yttrium manganite. *J. Mater. Res.*, 1994, **9**, 2645–2653.
9. Van der Pauw, L. J., A method of measuring specific resistivity and hall effect of discs of arbitrary shape. *Phil. Res. Rep.*, 1958, **13**, 1–9.
10. Dorris, S. E. and Mason, T. O., Electrical properties and cation valencies in Mn_3O_4. *J. Am. Ceram. Soc.*, 1988, **71**, 379–385.